

## SUPPORTING INFORMATION (SI)

### Experimental and Computational Study of the Exchange Interaction between the V(III) Centers in the Vanadium-Cyclal Dimer

Andreas Reiß<sup>[a]</sup>, Maximilian Kai Reimann<sup>[b]</sup>, Reinhard K. Kremer<sup>[c]</sup>, Rainer Pöttgen<sup>[b]</sup>, Chengyu Jin<sup>[d]</sup>, Karin Fink<sup>[d]</sup>, Martha Wachter-Lehn<sup>[e]</sup>, Wim Klopper<sup>[d,e]\*</sup>, and  
Claus Feldmann<sup>[a]\*</sup>

<sup>[a]</sup> *M.Sc. A. Reiß, Prof. Dr. C. Feldmann*

*Institut für Anorganische Chemie, Karlsruhe Institute of Technology (KIT),  
Engesserstraße 15, 76131 Karlsruhe, Germany  
claus.feldmann@kit.edu*

<sup>[b]</sup> *M.Sc. M. K. Reimann, Prof. Dr. R. Pöttgen*

*Institut für Anorganische und Analytische Chemie, WWU Münster,  
Corrensstraße 30, 48149 Münster, Germany*

<sup>[c]</sup> *Dr. R. K. Kremer*

*Max-Planck-Institut für Festkörperforschung,  
Heisenbergstraße 1, 70569 Stuttgart, Germany*

<sup>[d]</sup> *M.Sc. Chengyu Jin, Prof. Dr. K. Fink*

*Institut für Nanotechnology, Karlsruhe Institute of Technology (KIT),  
Hermann-von-Helmholtz-Platz 1, 76344 Eggenstein-Leopoldshafen, Germany*

<sup>[e]</sup> *B.Sc. Martha Wachter-Lehn, Prof. Dr. W. Klopper*

*Institut für Physikalische Chemie, Karlsruhe Institute of Technology (KIT),  
Fritz-Haber-Weg 2, 76131 Karlsruhe, Germany*

#### **Content**

**1. Analytical Techniques**

**2. Crystallographic Data**

**3. Computational Methods**

## 1. Analytical Techniques

**Transmission electron microscopy (TEM)** of the as-prepared V(0) nanoparticles was conducted using a FEI Osiris microscope, operating at an acceleration voltage of 200 kV. TEM samples were prepared by depositing a few drops of the V(0) nanoparticle suspension in THF on an amorphous carbon (Lacey-) film mounted on a 400  $\mu\text{m}$  mesh Cu grid (Plano). Thereafter, the sample holder was dried for two days under reduced pressure ( $< 10^{-3}$  mbar) to remove all volatiles (e.g., surface-adhered solvents). The sample holder was then transferred from a glovebox to the TEM microscope under strict exclusion of air and moisture using an air-tight transfer module (Gatan). The average particle diameter of the V(0) nanoparticles was calculated by statistical evaluation of at least 200 individual nanoparticles.

**Fourier-transformed infrared (FT-IR) spectroscopy.** FT-IR spectroscopy was performed on a Bruker Vertex 70. The spectrometer was equipped with a Platinum A 225 ATR unit (Bruker) with an air-tight sample chamber. Spectra of the V(0) nanoparticles and of **1** were analyzed using the OPUS program.

**X-ray powder diffraction (XRD)** was conducted on a Stoe Stadi MP, equipped with a Cu- $K_{\alpha}$  radiation source and a Ge-(111)-monochromator. For XRD analysis, the dried V(0) nanoparticles were mortared with an equal amount of glass powder (9-13  $\mu\text{m}$ , Sigma-Aldrich) to reduce the X-ray absorption of the sample. Thereafter, the resulting powdered mixture was transferred into a glass capillary (0.4 mm in diameter, Hilgenberg) for measurement.

**Elemental analysis (C/H/N analysis).** C/H/N analyses of the as-prepared V(0) nanoparticles and of **1** were performed on a Elementar Vario Micro Cube (Elementar, Germany) via complete thermal combustion of the respective sample at a temperature of 1,100  $^{\circ}\text{C}$  in an atmosphere of pure oxygen.

**Single-crystal X-ray diffraction and structure analysis.** Single-crystal X-ray diffraction with suitable single crystals of **1** was performed on an IPDS II diffractometer (Stoe) using Mo- $K_{\alpha}$  ( $\lambda = 7.1073 \text{ \AA}$ , graphite monochromator). For analysis, the single crystals were manually separated under an inert oil (perfluoropolyalkylether, ABCR) from the reaction mixture using a metal needle. Afterwards, the single crystal was mounted on a microgripper (MiTeGen) and measured thereafter at a temperature of 210 K.

Data reduction and multi-scan absorption correction were conducted by the X-AREA software package and Stoe LANA (version 1.75).<sup>S1</sup> Space group determination based on systematic absence of reflections was performed by XPREP. Using Olex2,<sup>S2</sup> the structures were solved with the ShelXS<sup>S3</sup>

structure solution program with Direct Methods and refined with the ShelXL<sup>S3</sup> refinement package using least squares minimization. All non-hydrogen atoms were refined anisotropically. Details of structure determination and structure refinement are listed in Table S1. DIAMOND was used for all illustrations.<sup>S4</sup> Refinement was checked with PLATON.<sup>S5</sup> Further details related to the crystal structures may be obtained from the joint CCDC/FIZ Karlsruhe deposition service on quoting the depository number 2289310.

**Magnetism.** Single crystals of  $[V_2(HCyclal)_2]$  were mechanically separated under an optical microscope in a glove box. Two different batches (sample masses of 6.100 mg and 7.229 mg, respectively) were studied with respect to their magnetic properties (temperature dependent susceptibility and magnetization measurements). The two batches were separately ground to fine powders inside a glove-box and filled into polypropylene capsules. The capsules were then attached to the brass sample holder rod of a vibrating sample magnetometer (VSM) of a Quantum Design Physical Property Measurement System (PPMS). The measurements were conducted in the temperature range of 2.5 to 300 K with applied external magnetic fields of up to 80 kOe. Fitting and plotting of the data was done with OriginPro 2016G.<sup>S6</sup>

## 2. Crystallographic Data

The unit cell of the title compound is shown in Figure S1. Crystallographic and refinement details of  $[V_2(HCyclal)_2]$  (**1**) are summarized in Table S1. A detailed analysis of the coordination around the vanadium centers points to a trigonal-bipyramidal coordination (Figure S2). Moreover, the two different positions of the azacrown ether are illustrated (Figure S3). The disorder is due to the different positions of the propyl unit in the azacrown ether. In addition to the first position of the molecular  $[V_2(HCyclal)_2]$  (*see main paper: Figure 3*), the V–N distances for the second position are 213.1(10) (N1) and 213.3(9) pm (N1') within the  $V_2N_2$  ring as well as 197.2(5) (N2), 187.2(12) (N3), and 220.4(7) pm (N4) to the non-bridging N atoms.

Structure and purity of the title compound were further confirmed by X-ray powder diffraction (Figure S4). Note that certain deviations between the experimental powder diffractogram (powder diffraction data recorded at room temperature/25 °C) and the calculated diffractogram (data of single crystal structure analysis recorded at 210 K) originate from the different temperatures of measurement.

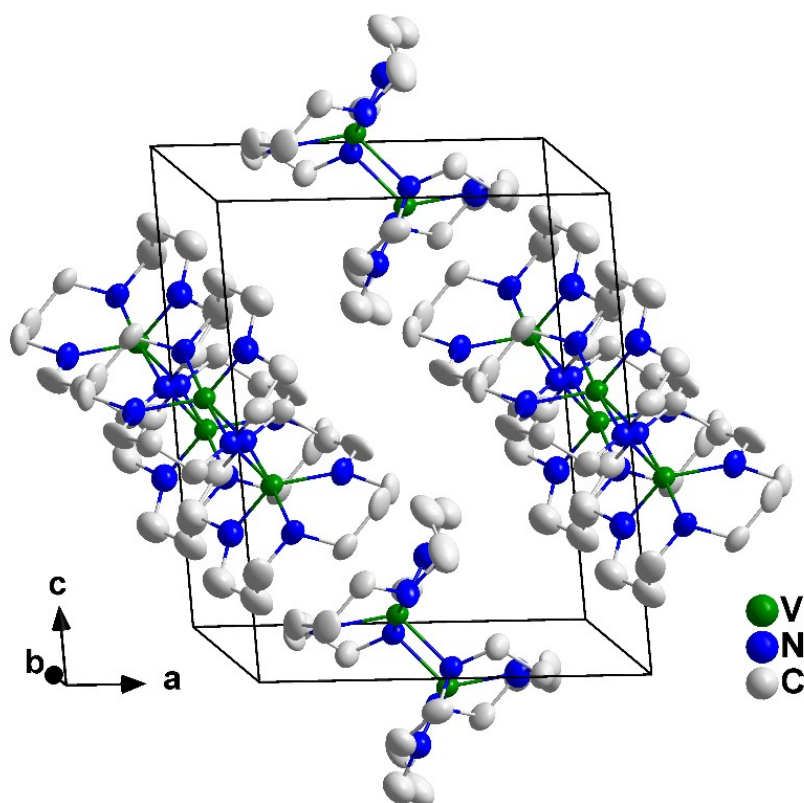


**Figure S1.** Unit cell of  $[\text{V}_2(\text{HCyclal})_2]$  (disorder of  $\text{H}_4\text{cyclal}$  and H atoms not shown for clarity).

**Table S1.** Crystallographic and refinement details of  $[\text{V}_2(\text{HCyclal})_2]$ .

<b>Data</b>	<b><math>[\text{V}_2(\text{HCyclal})_2]</math></b>
Sum formula	$\text{C}_{22}\text{H}_{46}\text{N}_8\text{V}_2$
Crystal system	monoclinic
Space group	$P2_1/n$
Lattice parameters	$a = 1105.0(4)$ pm
	$b = 850.8(2)$ pm
	$c = 1356.5(5)$ pm
	$\beta = 96.22(3)^\circ$
Cell volume	$V = 1267.8(7) \times 10^6$ pm <sup>3</sup>
Formula units per cell	$Z = 2$
Calculated density	$\rho = 1.374$ g cm <sup>-3</sup>
Measurement limits	$-13 \leq h \leq 13, -10 \leq k \leq 10, -16 \leq l \leq 16$
Theta range for data collection	2.26 to 26.00 °
Linear absorption coefficient	$\mu = 0.763$ mm <sup>-1</sup>
Number of reflections	8264 (2493 independent)
Refinement method	Full-matrix least-squares on $F^2$ for all
Merging	$R_{int} = 0.0662$
Number of parameters	280
Residual electron density	1.21 to $-0.43$ e <sup>-</sup> · 10 <sup>-6</sup> pm <sup>-3</sup>
$R1$ ( $I \geq 2\sigma_I$ )	0.0611
$R1$ (all data)	0.0660
$wR2$ (all data)	0.1721
Goof	1.072

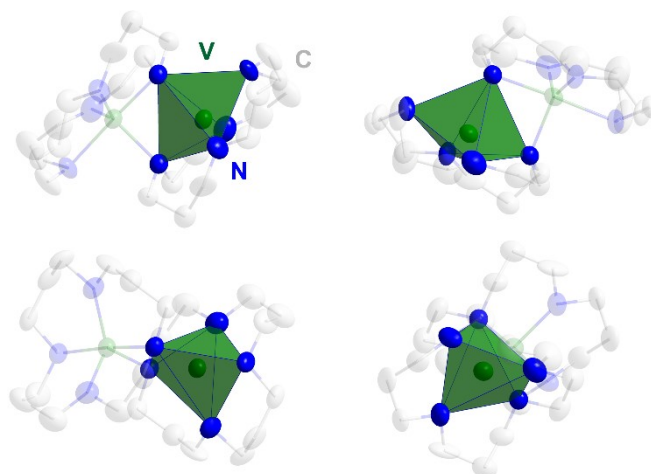


**Figure S2.** Distorted trigonal-bipyramidal coordination around the vanadium center with different views on the  $\text{VN}_6$  polyhedron.

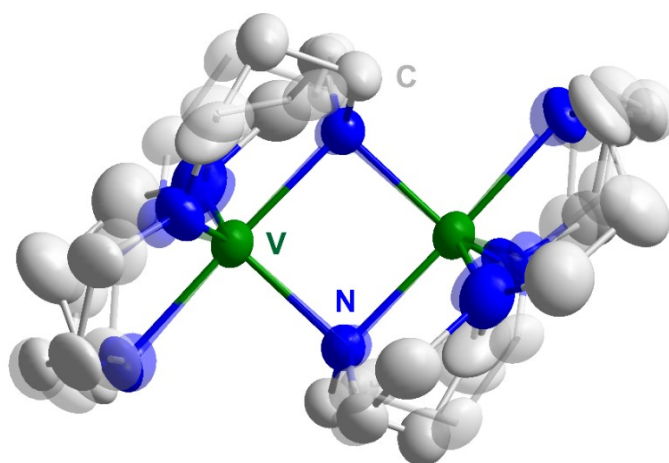


**Figure S3.** Molecular structure of  $[\text{V}_2(\text{HCyclal})_2]$  with both positions of the disordered azacrown ether (H atoms not shown for clarity).

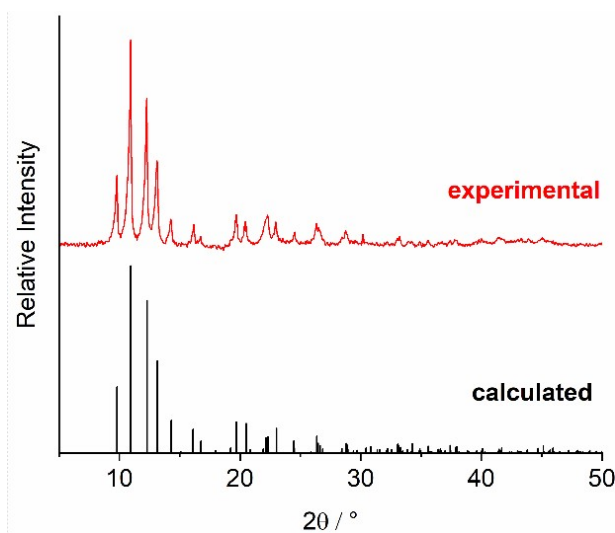


**Figure S4.** X-ray powder diffraction of  $[\text{V}_2(\text{HCyclal})_2]$  (data recorded at 25 °C) and comparison to diffractogram calculated based on the data of the single-crystal structure analysis (data recorded at 210 K).

### 3. Computational Methods

The DFT calculations were performed with the TURBOMOLE program package (version V7.5.1).<sup>S7</sup> The global hybrid functionals B3LYP<sup>S8</sup> and TPSSh<sup>S9</sup> were investigated. For the V and N atoms, we used the def2-TZVPP basis of Gaussian atomic orbitals, while the smaller def2-TZVP and def2-SV(P) basis sets were used for C and H, respectively.<sup>S10</sup> TURBOMOLE's grid 5 (*gridsize 5*) was used for numerical integration, and weight derivatives were taken into account when computing analytic nuclear gradients. The D3(BJ) dispersion correction<sup>S11</sup> including the three-body term (*\$disp3 bj-abc*) was added to the DFT energies.

All DFT energies were converged to within  $10^{-11} E_h$  (*\$scfconv 11 and \$denconv 1d-10*), and the geometry optimizations were carried out until the maximum norm of the gradient was smaller than  $10^{-6} E_h/a_0$  (*jobex-energy 9-gcart 6*). A small script was written to combine the energies and gradients from two calculations into one data set to be used for the geometry optimization.

Localized molecular orbitals were determined using the approach of Pipek and Mezey (*\$localize pipmez*).<sup>S12</sup>

Cartesian coordinates of  $[V_2(\text{HCyclal})_2]$  as obtained at the B3LYP-D3(BJ)-abc level and the TPSSh-D3(BJ)-abc level are listed in Tables S2 and S3, respectively.

**Table S2.** Cartesian coordinates (in Å) of  $[V_2(\text{HCyclal})_2]$  as obtained at the B3LYP-D3(BJ)-abc level (basis set: V = def2-TZVPP, N = def2-TZVPP, C = def2-TZVP, H = def2-SV(P)).

V	-0.8335347	-0.5096252	1.1473308
N	-0.9635860	-2.5148668	2.2043715
H	-0.5412260	-3.1005576	1.4797954
N	-2.7485469	-0.4779993	0.7731065
N	-0.4307741	1.4004071	0.2529131
N	0.2165974	0.2201035	2.5967190
C	-2.3245447	-3.0317676	2.4109508
H	-2.2727935	-4.0718513	2.7729567
H	-2.8063341	-2.4286074	3.1900335
C	-3.1246310	-2.9526213	1.1279907
H	-3.9661311	-3.6539273	1.1924526
H	-2.4967984	-3.2829724	0.2886579
C	-3.6948807	-1.5762427	0.8496203
H	-4.4572534	-1.3671231	1.6303294
H	-4.2553377	-1.6403840	-0.1041174
C	-3.5242295	0.6848861	0.3672442
H	-4.4473990	0.7399988	0.9762403
H	-3.8626293	0.5547549	-0.6832856
C	-2.8278111	2.0252481	0.4710665
H	-2.5951839	2.2394658	1.5218079
H	-3.5331924	2.7948193	0.1272990
C	-1.5607624	2.0878643	-0.3692987
H	-1.7729058	1.6176417	-1.3375081
H	-1.3063417	3.1480883	-0.5654026
C	0.1586964	2.2429334	1.2928133
H	-0.6404960	2.7231752	1.8773546
H	0.7749945	3.0572359	0.8668961
C	0.9804050	1.4062023	2.2470699

H	1.2130692	2.0129478	3.1396145
H	1.9472212	1.1382944	1.7797202
C	0.5810130	-0.2836762	3.8942806
H	0.4951368	0.5166871	4.6545910
H	1.6477826	-0.6022583	3.9078490
C	-0.2606412	-1.4630316	4.3455478
H	0.0636352	-1.7602180	5.3508768
H	-1.3134253	-1.1563774	4.4151425
C	-0.1351214	-2.6587931	3.4181151
H	-0.4207268	-3.5845565	3.9428295
H	0.9093585	-2.7607401	3.1049257
V	0.8335347	0.5096252	-1.1473308
N	0.9635860	2.5148668	-2.2043715
H	0.5412260	3.1005576	-1.4797954
N	2.7485469	0.4779993	-0.7731065
N	0.4307741	-1.4004071	-0.2529131
N	-0.2165974	-0.2201035	-2.5967190
C	2.3245447	3.0317676	-2.4109508
H	2.2727935	4.0718513	-2.7729567
H	2.8063341	2.4286074	-3.1900335
C	3.1246310	2.9526213	-1.1279907
H	3.9661311	3.6539273	-1.1924526
H	2.4967984	3.2829724	-0.2886579
C	3.6948807	1.5762427	-0.8496203
H	4.4572534	1.3671231	-1.6303294
H	4.2553377	1.6403840	0.1041174
C	3.5242295	-0.6848861	-0.3672442
H	4.4473990	-0.7399988	-0.9762403
H	3.8626293	-0.5547549	0.6832856
C	2.8278111	-2.0252481	-0.4710665
H	2.5951839	-2.2394658	-1.5218079
H	3.5331924	-2.7948193	-0.1272990
C	1.5607624	-2.0878643	0.3692987
H	1.7729058	-1.6176417	1.3375081
H	1.3063417	-3.1480883	0.5654026
C	-0.1586964	-2.2429334	-1.2928133
H	0.6404960	-2.7231752	-1.8773546
H	-0.7749945	-3.0572359	-0.8668961
C	-0.9804050	-1.4062023	-2.2470699
H	-1.2130692	-2.0129478	-3.1396145
H	-1.9472212	-1.1382944	-1.7797202
C	-0.5810130	0.2836762	-3.8942806
H	-0.4951368	-0.5166871	-4.6545910
H	-1.6477826	0.6022583	-3.9078490
C	0.2606412	1.4630316	-4.3455478
H	-0.0636352	1.7602180	-5.3508768
H	1.3134253	1.1563774	-4.4151425
C	0.1351214	2.6587931	-3.4181151
H	0.4207268	3.5845565	-3.9428295
H	-0.9093585	2.7607401	-3.1049257

**Table S3.** Cartesian coordinates (in Å) of  $[V_2(\text{HCyclal})_2]$  as obtained at the TPSSh-D3(BJ)-abc level (basis set: V = def2-TZVPP, N = def2-TZVPP, C = def2-TZVP, H = def2-SV(P)).

V	-0.7932396	-0.4877756	1.1022645
N	-0.9320606	-2.4707917	2.1609125
H	-0.5001276	-3.0582375	1.4392465
N	-2.7097776	-0.4460582	0.7516549
N	-0.4434214	1.4282441	0.2672499
N	0.2588783	0.2236039	2.5507124

C	-2.2894606	-3.0045577	2.3656086
H	-2.2240785	-4.0470883	2.7254722
H	-2.7777701	-2.4059123	3.1467630
C	-3.0809722	-2.9250559	1.0772325
H	-3.9190892	-3.6352330	1.1284321
H	-2.4414442	-3.2407005	0.2386111
C	-3.6573466	-1.5484827	0.8152385
H	-4.4188510	-1.3472204	1.6012676
H	-4.2187336	-1.5969193	-0.1411016
C	-3.5139730	0.7151023	0.3888666
H	-4.4229834	0.7399024	1.0244860
H	-3.8764620	0.5999608	-0.6570051
C	-2.8258689	2.0576822	0.5060243
H	-2.5714502	2.2526643	1.5577317
H	-3.5397018	2.8334078	0.1870359
C	-1.5720456	2.1233451	-0.3531533
H	-1.7884900	1.6470393	-1.3200919
H	-1.3111421	3.1847847	-0.5485052
C	0.1450902	2.2733007	1.3073186
H	-0.6590978	2.7217566	1.9146287
H	0.7290544	3.1119579	0.8765069
C	1.0042508	1.4337528	2.2245806
H	1.2372814	2.0179698	3.1338860
H	1.9662397	1.1914462	1.7334601
C	0.5775560	-0.2470464	3.8764040
H	0.4532743	0.5730224	4.6127045
H	1.6459251	-0.5570770	3.9382140
C	-0.2775150	-1.4225109	4.3112539
H	0.0142882	-1.7155506	5.3301454
H	-1.3344802	-1.1169228	4.3414118
C	-0.1159101	-2.6160668	3.3860819
H	-0.4011780	-3.5511824	3.8992171
H	0.9357105	-2.7018010	3.0854138
V	0.7932396	0.4877756	-1.1022645
N	0.9320606	2.4707917	-2.1609125
H	0.5001276	3.0582375	-1.4392465
N	2.7097776	0.4460582	-0.7516549
N	0.4434214	-1.4282441	-0.2672499
N	-0.2588783	-0.2236039	-2.5507124
C	2.2894606	3.0045577	-2.3656086
H	2.2240785	4.0470883	-2.7254722
H	2.7777701	2.4059123	-3.1467630
C	3.0809722	2.9250559	-1.0772325
H	3.9190892	3.6352330	-1.1284321
H	2.4414442	3.2407005	-0.2386111
C	3.6573466	1.5484827	-0.8152385
H	4.4188510	1.3472204	-1.6012676
H	4.2187336	1.5969193	0.1411016
C	3.5139730	-0.7151023	-0.3888666
H	4.4229834	-0.7399024	-1.0244860
H	3.8764620	-0.5999608	0.6570051
C	2.8258689	-2.0576822	-0.5060243
H	2.5714502	-2.2526643	-1.5577317
H	3.5397018	-2.8334078	-0.1870359
C	1.5720456	-2.1233451	0.3531533
H	1.7884900	-1.6470393	1.3200919
H	1.3111421	-3.1847847	0.5485052
C	-0.1450902	-2.2733007	-1.3073186
H	0.6590978	-2.7217566	-1.9146287
H	-0.7290544	-3.1119579	-0.8765069
C	-1.0042508	-1.4337528	-2.2245806
H	-1.2372814	-2.0179698	-3.1338860
H	-1.9662397	-1.1914462	-1.7334601

C	-0.5775560	0.2470464	-3.8764040
H	-0.4532743	-0.5730224	-4.6127045
H	-1.6459251	0.5570770	-3.9382140
C	0.2775150	1.4225109	-4.3112539
H	-0.0142882	1.7155506	-5.3301454
H	1.3344802	1.1169228	-4.3414118
C	0.1159101	2.6160668	-3.3860819
H	0.4011780	3.5511824	-3.8992171
H	-0.9357105	2.7018010	-3.0854138

---

Based on the B3LYP-D3(BJ)-abc optimized structure of the singlet state, complete-active-space self-consistent field (CASSCF)<sup>S13</sup> and complete-active-space spin-orbit configuration-interaction calculations (CASOCI)<sup>S14</sup> were performed in an active space containing the two singly occupied  $3d$  electrons at each vanadium atom (Table S4). In the calculations, a def2-SVP basis was used for C and H and a def2-TZVP basis set for N and V. At the CASSCF level, the magnetic exchange coupling is much too small. The main reason is that charge-transfer states are described by the orbitals for the neutral system. The influence of orbital relaxation effects in the charge-transfer configurations on the magnetic exchange coupling is considered by shifting down the energies of all determinants describing charge-transfer states.<sup>S15</sup> The relaxation energies were calculated for one half of the molecule. Orbitals were first optimized for a triplet state (neutral). Starting from these orbitals, the energy differences for the ions in the first iteration of a self-consistent-field (SCF) calculation and after orbital relaxation was taken as relaxation energy. The calculations yielded an exchange-coupling constant of  $-247$  K ( $-60$  K without relaxation effects). The way, the relaxation energy is computed, is an approximation. Changing it to 0.4 hartree and 0.45 hartree yielded exchange-coupling constants of  $-220$  K and  $-300$  K, respectively. The magnetic susceptibility was obtained by Boltzmann averaging of the magnetic moments (Figure S5). Assuming a paramagnetic impurity from a potential V(III) monomer in a triplet state, an amount of 6 % was obtained from the low-temperature behaviour of the experimental susceptibility curve. At high temperatures, the calculated magnetic susceptibility is a bit too high indicating that the exchange coupling is slightly underestimated. Therefore,  $J$  was fitted to the experimental data with the program package PHI,<sup>S16</sup> keeping the paramagnetic impurity constant. From this fit, an exchange coupling constant of  $-289$  K was obtained.

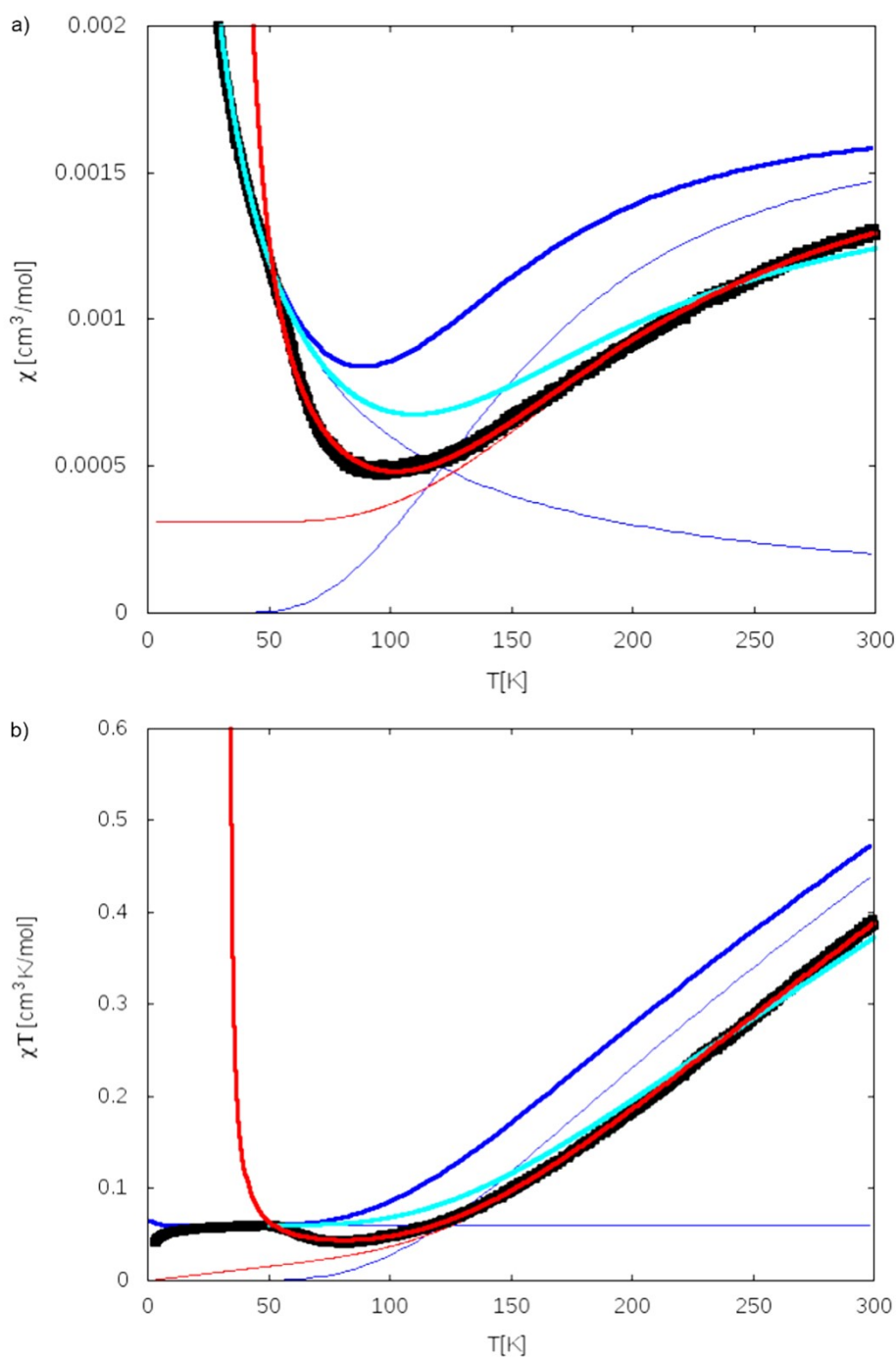


**Figure S5.** Simulation of the magnetic susceptibility with a)  $\chi$  versus  $T$  (top) and b)  $\chi T$  versus  $T$ : experimental data (black dots); fitted with eq. (1a)-(1d) in the main manuscript without magnetic impurity (thin red line) and with an additional Curie term considering a magnetic impurity at low temperatures magnetic impurity (thick red line). The line starting at zero shows the magnetic susceptibility calculated directly from the CASOCI wave functions and energies (thin blue lines) with the second thin blue line representing a paramagnetic impurity of a triplet state with a weight of 6 % (fitted to the measured low temperature value); Weighted sum of the latter two curves (6 % paramagnetic impurity and 94 % calculated susceptibility, fat blue line). Only  $J$ -fitted with the

program package PHI with the Heisenberg Hamiltonian  $-2J S_1 S_2$  and the paramagnetic impurity of 6 % (turquoise line).

**Table S4.** CASOCI energies in hartree and K of the exchange-coupled  $S^T = 0$ ,  $S^T = 1$ , and  $S^T = 2$  states calculated with a shift of the charge-transfer determinants by  $-0.4219144245$  hartree ( $-11.48$  eV).

State	Energy [hartree]	Energy/ $k_B$ [K]
1:	-3190.7809658536071	0.00
2:	-3190.7794876187018	466.81
3:	-3190.7794876150565	466.81
4:	-3190.7794828784808	468.31
5:	-3190.7762314006927	1495.10
6:	-3190.7762297304557	1495.62
7:	-3190.7762297264248	1495.62
8:	-3190.7762246974917	1497.21
9:	-3190.7762246974912	1497.21

( $J = -247$  K)

In spin only cases, generally,  $\chi^T = \frac{g^2 S(S+1)}{8}$  is with  $g = 2$ . Moreover,  $\chi^T = 0$  cm<sup>3</sup>K/mol relates to a singlet state,  $\chi^T = 1$  cm<sup>3</sup>K/mol for a triplet state, and  $\chi^T = 3$  cm<sup>3</sup>K/mol for a quintet state. The V(III) centres in  $[V_2(\text{HCyclal})_2]$  are strongly antiferromagnetically coupled to a singlet ground state, a triplet excited state at  $E = -2J$  and a quintet state at  $E = -6J$ . Because of the singlet ground state,  $\chi^T = 0$  cm<sup>3</sup>K/mol is expected at low temperatures. Nevertheless, the experimental  $\chi^T$  value amounts to a rather constant value of 0.06 cm<sup>3</sup>K/mol in the temperature range from 15 K and 50 K. This can be assigned to a paramagnetic impurity. Assuming a triplet impurity, this corresponds to about 6 % of the impurity (most likely the respective monomer of the title compound). The temperature-dependent contribution of the three different spin states of  $[V_2(\text{HCyclal})_2]$  to  $\chi^T$  is given by the Boltzmann distribution. For given  $J$  and  $T$ , the probability of the different spin states of the dimer are:

$$p(S^T = 0) = \frac{1}{1 + 3 * \exp\left(2 * \frac{J}{k_B T}\right) + 5 * \exp\left(6 * \frac{J}{k_B T}\right)}$$

$$p(S^T = 1) = \frac{3 * \exp\left(2 * \frac{J}{k_B T}\right)}{1 + 3 * \exp\left(2 * \frac{J}{k_B T}\right) + 5 * \exp\left(6 * \frac{J}{k_B T}\right)}$$

$$p(S^T = 2) = \frac{5 * \exp\left(6 * \frac{J}{k_B T}\right)}{1 + 3 * \exp\left(2 * \frac{J}{k_B T}\right) + 5 * \exp\left(6 * \frac{J}{k_B T}\right)}$$

The resulting contributions of the different spin states are given in Table S5. Taking the values for  $J = -289$  K, 69 % of the  $[V_2(\text{HCyclal})_2]$  molecules are in the singlet ground state, 30 % in the triplet state and 1 % in the quintet state at 300 K. This corresponds to  $\chi^T = 0.34$  cm<sup>3</sup>K/mol. Combining with 6 % of a paramagnetic impurity and 94 % of  $V_2(\text{HCyclal})_2$ ,  $\chi^T = 0.38$  cm<sup>3</sup>K/mol, is in good agreement with the experimental value. Due to the fact that only about 30 % of the  $[V_2(\text{HCyclal})_2]$  molecules are not in the singlet state, this value is rather low compared to the theoretical limit at very high temperatures, which corresponds to  $\chi^T = 2$  cm<sup>3</sup>K/mol, being two times the value of a triplet state. Because of the strong coupling, this value is only reached at temperatures of several thousand K. The value obtained for  $J$  is slightly method dependent. However, the spin-state distributions for  $J = -300$  K and  $J = -289$  K are very similar.

**Table S5.** Distribution of the spin states of  $[V_2(\text{HCyclal})_2]$  (%) for different coupling constants and temperatures and the corresponding  $\chi^T$  value (cm<sup>3</sup>K/mol).

$J$ [K]	289			$\chi^T$	300			$\chi^T$
T [K]	singlet	triplet	quintet		singlet	triplet	quintet	
0	100.0	0.0	0.0	0	100.0	0.0	0.0	0
100	99.1	0.9	0.0	0.009	99.3	0.7	0.0	0.007
300	68.9	30.1	1.1	0.334	70.5	28.6	0.9	0.331
10000	12.4	35.2	52.3	1.921	12.5	35.3	52.2	1.919

## References

- (S1) X-RED32, Data Reduction Program (Version 1.01). Stoe, Darmstadt **2001**.
- (S2) O. V. Dolomanov, L. J. Bourhis, R. J. Gildea, J. A. K. Howard and H. Puschmann, *J. Appl. Crystallogr.*, 2009, **42**, 339-341.
- (S3) G. M. Sheldrick, *Acta Crystallogr. A*, 2008, **64**, 112-122.
- (S4) DIAMOND (Version 4.2.2): *Crystal and Molecular Structure Visualization*. Crystal Impact GbR, Bonn 2016.
- (S5) G. M. Sheldrick, *Acta Crystallogr. C*, 2015, **71**, 3-8.
- (S6) OriginLab Corp. OriginPro 2016G (version 9.3.2.303), 2016.
- (S7) TURBOMOLE V7.5.1 2021: A development of University of Karlsruhe and Forschungszentrum Karlsruhe GmbH, 1989-2007, TURBOMOLE GmbH, since 2007; available from <https://www.turbomole.org>.
- (S8) P. J. Stephens, F. J. Devlin, C. F. Chabalowski and M. J. Frisch, *J. Phys. Chem.*, 1994, **98**, 11623-11627
- (S9) V. N. Staroverov, G. E. Scuseria, J. Tao and J. P. Perdew, *J. Chem. Phys.*, 2003, **119**, 12129-12137; Erratum, *ibid.* 2004, **121**, 11507.

- (S10) F. Weigend and R. Ahlrichs, *Phys. Chem. Chem. Phys.*, 2005, **7**, 3297-3305.
- (S11) S. Grimme, S. Ehrlich and L. Goerigk, *J. Comput. Chem.*, 2011, **32**, 1456-1465.
- (S12) J. Pipek and P. G. Mezey, *J. Chem. Phys.*, 1989, **90**, 4916-4926.
- (S13) U. Meier and V. Staemmler, *Theor. Chim. Acta*, 1989, **76**, 95-111.
- (S14) T. Bodenstein, A. Heimermann, K. Fink and C. van Wüllen, *ChemPhysChem*, 2022, **23**, e202100648.
- (S15) K. Fink and V. Staemmler, *Mol. Phys.*, 2013, **111**, 2594-2605.
- (S16) N. F. Chilton, R. P. Anderson, L. D. Turner, A. Soncini and K. S. Murray, *J. Comput. Chem.*, 2013, **34**, 1164-1175.